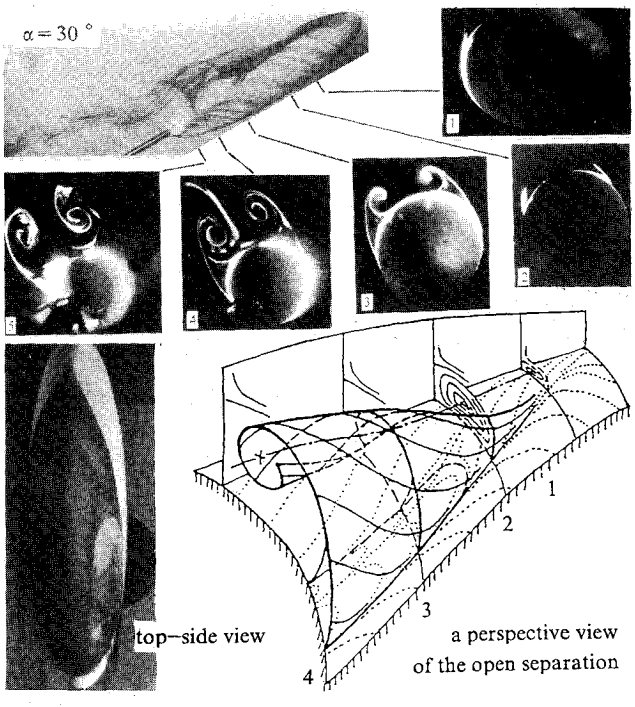

Fig. 3 Features of the open separation and the vortex formation.

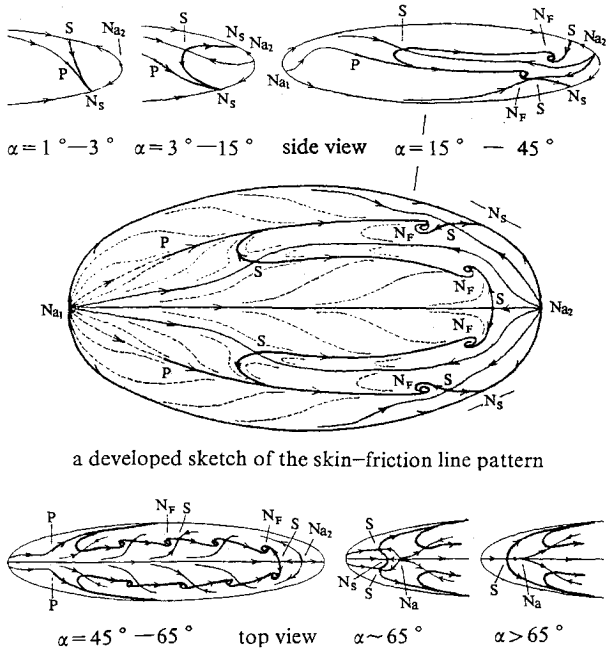

Fig. 4 Topological structures of the separated flows and their evolution with changing α.

primary separation line rolls up into a concentrated vortex above the body. The outer boundary of the bubble becomes the aft segment of the primary separation line, and so only the fore segment of it is the open separation line practically. In the α region of 45–65 deg, the vortex bursts above the body and is called a bursting vortex. The flowfield becomes unsteady and asymmetric. At about 65 deg, the two open separation lines join up and become a closed separation line. There is another type of vortex: the vertical vortex shed from the aft segments of the primary and secondary separation line (see the photo of α = 30 deg). It is very weak and unsteady. When α > 65 deg, the flow becomes unsteady vortex shedding (see α = 70 deg). Figure 3 gives some results from the laser sheet technique. It can be seen that the free edge of the separation surface from open separation is a spiral streamline, which is around the vortex axis instead of coinciding with it.

3) The topological property and identification of the starting point of open separation: Figures 1–3 show that there is not any singular point in the starting region of an open separation, including the body surface and the flowfield concerned. However, we have found that the open separation leads to a fold of the near-wall stream surface; it is just a cusp catastrophe, and the cusp point on the wall can be used to define and identify the starting point of open separation.[4]

4) The topological structures of the separated flow and their evolution with changing α are shown in Fig. 4. It is from a topological analysis to the experimental results obtained. In Fig. 4, P–N_S (or P–N_F) denotes the open separation line, and S–N_S (or S–N_F) denotes the closed separation line. The N_F is the footprint of the vertical vortex. The developed sketch of a surface flow pattern can be obtained by cutting the body surface from N_{a_1} to N_{a_2} and developing it in a topological manner. In the α region of 45–65 deg, there are several unsteady pairs of N_F–S on the secondary separation line. The theoretic foundation of the previous topological analysis is in Ref. 5.

Acknowledgment

This investigation was sponsored by the National Natural Science Foundation of China.

References

[1]Costis, C. E., Hoang, N. T., and Telionis, D. P., "Laminar Separating Flow over a Prolate Spheroid," *Journal of Aircraft,* Vol. 26, No. 9, 1989, pp. 810–816.

[2]Wang, K. C., Zhou, H. C., Hu, C. H., and Harrinton, S., "Three-Dimensional Separated Flow Structure over Prolate Spheroids," *Proceedings of the Royal Society of London, Series A, Mathematical and Physical Sciences,* Vol. 421, 1990, pp. 73–90.

[3]Su, W., Tao, B., and Xu, L., "Experimental Investigation of Three-Dimensional Separated Flow over a Prolate Spheroid," *Recent Advances in Experimental Fluid Mechanics, Proceedings of the 1st International Conference on Experimental Fluid Mechanics,* edited by F. G. Zhuang, International Academic Publishers, Beijing, People's Republic of China, 1992, pp. 205–210.

[4]Su, W., and Tao, B., "Topological Properties of Three-Dimensional Boundary Layer and Three-Dimensional Separation," *Proceedings of the 2nd International Conference on Fluid Mechanics,* (Beijing, People's Republic of China), Peking Univ. Press, Beijing, People's Republic of China, 1993, pp. 539–544.

[5]Lighthill, M. J., "Attachment and Separation in Three-Dimensional Flow," *Laminar Boundary-Layers,* Vol. II 2.6, edited by L. Rosenhead, Oxford Univ. Press, Oxford, England, UK, 1963, pp. 72–82.

Reynolds Stress Profiles in the Near Wake of an Oscillating Airfoil

Seung O. Park* and Boo Il Lee†
Korea Advanced Institute of Science and Technology, Taejon 305-701, Republic of Korea

Introduction

MOST previous research efforts concerning unsteady aerodynamics of oscillating airfoils were directed to unsteady wing loading associated with separation and dynamic stall phenomena. Relatively little attention, however, has been given to the study of oscillating wakes. Ho and Chen[1] studied experimentally the unsteady wake of a plunging airfoil at incidence using a hot-wire rake. De Ruyck and Hirsch[2] measured the instantaneous velocity

Received Oct. 30, 1992; revision received March 26, 1993; accepted for publication April 2, 1993.

*Professor, Department of Aerospace Engineering. Member AIAA.
†Research Assistant, Department of Aerospace Engineeing.

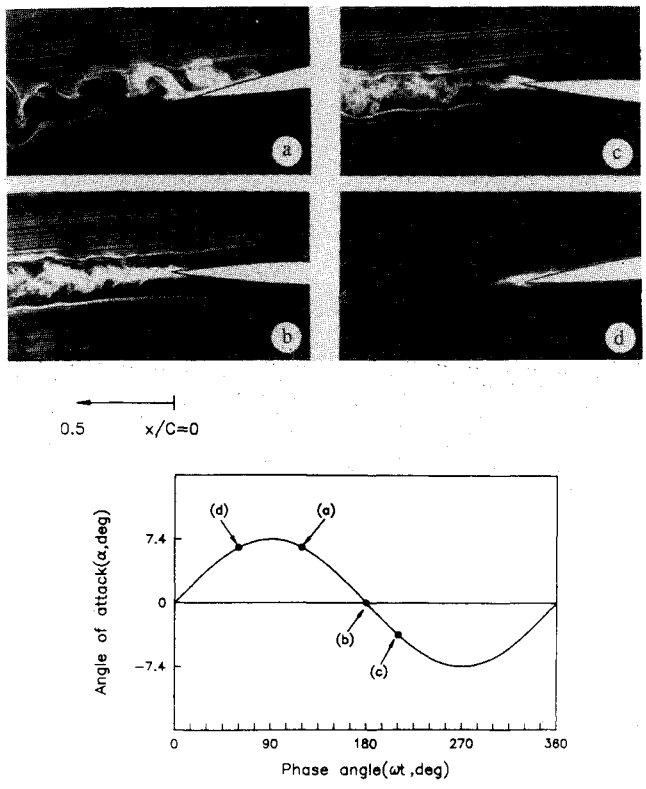

Fig. 1 Wake visualization K = 0.2, flow right to left: a) α = 6.4 deg, ωt = 120 deg; b) α = 0 deg, ωt = 180 deg; c) α = −3.7 deg, ωt = 210 deg; and d) α = 6.4 deg, ωt = 60 deg.

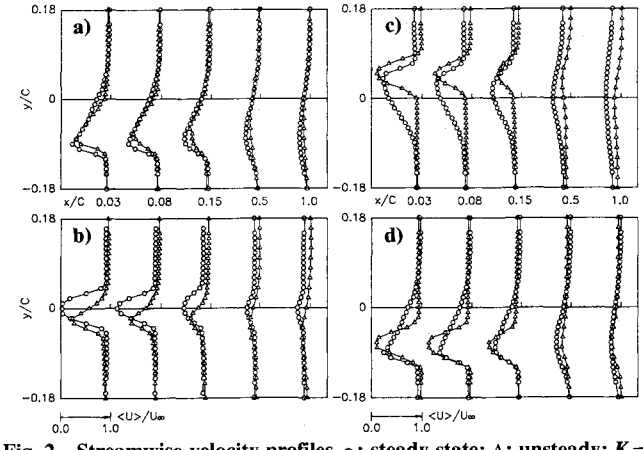

Fig. 2 Streamwise velocity profiles ○: steady state; Δ: unsteady; K = 0.2: a) α = 6.4 deg, ωt = 120 deg; b) α = 0 deg, ωt = 180 deg; c) α = −3.7 deg, ωt = 210 deg; and d) α = 6.4 deg, ωt = 60 deg.

and turbulence intensity profiles of the wake of a sinusoidally pitching airfoil.

In our previous work,[3,4] we studied experimentally unsteady wakes behind an airfoil oscillating in pitch about several mean incidences. The phase-averaged velocity and turbulence intensity profiles were measured with a stationary I-type hot wire and the periodic variation of the wakes was visualized using a smoke-wire technique. As an extension to our earlier work, measurements of the turbulence quantities using an X-type hot wire in the near wake were carried out. The unsteady wake of the present work undergoes various states of change. Depending on the phase angle of oscillation, the wake may exhibit very well organized vortical structures, or it may show intermingled, fully turbulent features. The purpose of the present Note is to report the Reynolds stress distributions at several downstream stations in conjunction with the visualized wake. This will enhance our understanding of the link between the Reynolds stress profiles and the wake flow patterns often represented by streak lines.

Experiments

The experimental setup used for the present study was the same as the one reported earlier.[4] The mean incidence angle and the amplitude of oscillation were set at 0 and 7.4 deg, respectively. The reduced frequency K, defined as $K = \omega C/2U_\infty$, was 0.2. Here, ω is the circular frequency, C the chord length, and U_∞ the free-stream velocity. U_∞ was set at 4 m/s and the Reynolds number based on the chord length was 27,000.

A Dantec constant temperature hot-wire anemometer system (type 55M10) along with an X-type probe (type 55P61) were employed for measurements. Two TSI model 1072 linearizers were utilized to linearize the anemometer output from each channel. To monitor the temperature variation during the measurement, a T-type thermocouple (Fluke 2190A) was installed in the test section.

The trigger pulse produced once per revolution of the driving disk was sent to the Waveform Analyzer (DATA 6000, Data Precision Co.) equipped with a 14-bit analog-to-digital converter. Data were taken, at a given probe location, at 48 sampling points (48 phase angles) distributed evenly over a period of oscillation. For each phase angle, 300 ensembles were used for averaging. Measurements were made at five downstream stations: x/C = 0.03, 0.08, 0.15, 0.5, and 1.0. At all of the stations, the probe was traversed vertically in the range y/C = −0.4–0.4.

To minimize the temperature variation during the measurement, the system was warmed up long enough to maintain laboratory room temperature approximately constant within ±1 deg. To account for the temperature change in the test section during measurement, the output voltage was corrected based on the formula of Kanevce and Oka.[5] To compensate the output voltage for the velocity component parallel to the axis of the wire, we adopted the formula suggested by Champagne and Sleicher.[6]

The flow visualization photographs were taken in our earlier work[3] and some of those are reproduced here for convenience of the presentation of the present measurement data.

Results and Discussion

Figures 1a–1d show some of the wake flow patterns that appear during the period of oscillation. Since the Reynolds number of the present experiment was rather small, the near wake was not always turbulent. The hot-wire signal monitored at x/C = 0.03 indicated that the wake at this location varied from wavy to turbulent flow. The output signals for the phase angle in the range of 30–70 deg and 210–300 deg showed that the flow was wavy (see Fig. 1d). Corresponding to each plate of Fig. 1, the mean streamwise velocity, the streamwise and the transverse intensity, and the shear stress profiles are given in Figs. 2, 3, and 4, respectively. For reference purposes, the velocity and the shear stress profiles for the

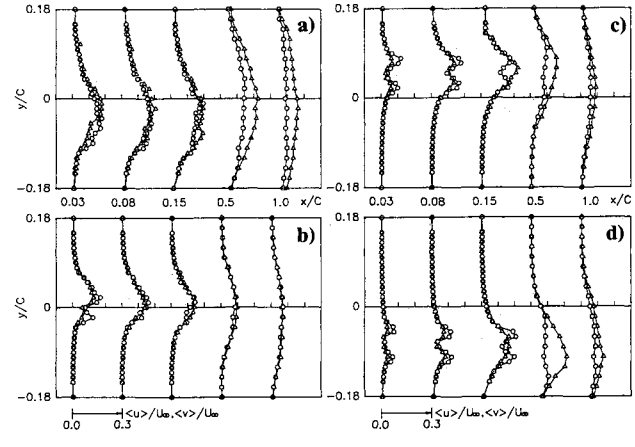

Fig. 3 Turbulence intensity profiles, unsteady, ○: streamwise intensity; Δ: transverse intensity; K = 0.2: a) α = 6.4 deg, ωt = 120 deg; b) α = 0 deg, ωt = 180 deg; c) α = −3.7 deg, ωt = 210 deg; and d) α = 6.4 deg, ωt = 60 deg.

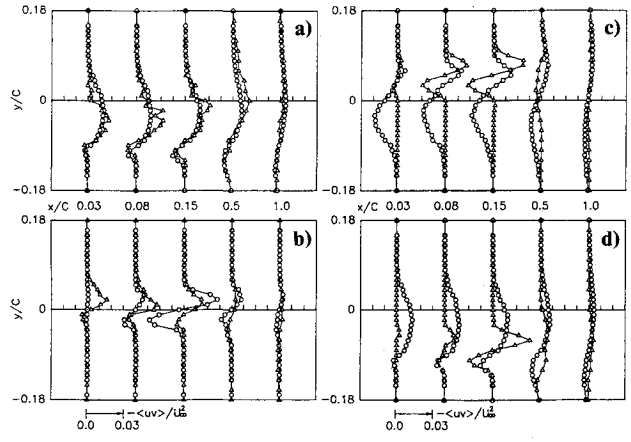

Fig. 4 Reynolds shear stress profiles ○: steady state; Δ: unsteady; K = 0.2: a) α = 6.4 deg, ωt = 120 deg; b) α = 0 deg, ωt = 180 deg; c) α = −3.7 deg, ωt = 210 deg; and d) α = 6.4 deg, ωt = 60 deg.

case of the steady airfoil measured at the same angle of attack as the instantaneous angle of attack of the pitching airfoil are included in Figs. 2 and 4, respectively.

Figure 1a illustrates shed-off turbulent vortices after the onset of trailing-edge separation. The corresponding velocity profiles and the Reynolds stress profiles are shown in Figs. 2a, 3a, and 4a, respectively. The velocity profiles in the very near wake (x/C < 0.2) of Fig. 2a indicate that the wake thickness at this instant is considerably larger than the other cases. The turbulence intensity profiles seen in Fig. 3a are broader and the intensity levels are higher than in the other cases. In the very near wake region, the streamwise and the transverse intensity profiles are roughly the same. The Reynolds stress profiles of Fig. 4a indicate that the shear stress in the upper part of the wake is much larger than in the lower part reflecting the large-scale turbulent vortical structures shedding off the upper surface and the subsequent bursting of those structures into the wake.

As the instantaneous angle of attack decreases further, the wake becomes fully turbulent and narrower. A typical flow pattern at zero instantaneous angle of attack is shown in Fig. 1b. The velocity profiles of Fig. 2b and the intensity profiles of Fig. 3b clearly demonstrate that the wake thickness has become much smaller than that for the case of Fig. 1a. The shear stress profiles corresponding to this case (Fig. 4b) are in close resemblance to those of a steady flat-plate turbulent wake at a small incidence. We note that the peak value of the upper part of the wake is larger than that of the lower part and that the upper wake is thicker than the lower wake.

Figure 1c illustrates the wake profile undergoing transition from fully turbulent (Fig. 1b) to wavy wake (Fig. 1d). The turbulent intensity profiles of Fig. 3c and those of Fig. 3b at x/C = 0.03 show that the profiles are double peaked reflecting the boundary layers developed over the upper and the lower surfaces of the airfoil. The peak values of the turbulence intensities (Fig. 3c) and the shear stress (Fig. 4c) are seen to increase with downstream distance up to x/C = 0.15. It is interesting to note that the shear stress profiles at x/C = 0.08 and 0.15 are nearly symmetric about the wake centerline. Also, the magnitude of the peak values at these two stations are much larger than those of Fig. 4b where the instantaneous angle of attack was zero and the wake appeared to be fully turbulent.

When the instantaneous angle of attack increases further, the wake flow pattern becomes wavy and resembles the Karman vortex street. A typical flow pattern is given in Fig. 1d. The intensity profiles for this case (Fig. 3d) are seen to be qualitatively similar to those of Fig. 3c. In the very near wake region, both the streamwise and the transverse intensity profiles have double peaks, and the peak value increases with downstream distance. It is noted that the double peaks of the transverse intensity profiles disappear earlier than those of the streamwise profiles (this is also seen in Fig. 3c). We conjecture that the diffusion of the transverse intensity becomes greater as a result of the vertical up-and-down motion of the trailing edge. When the intensity profiles of Figs. 3c and 3d are compared to those of Fig. 3a, we find that the distinct double peaks normally appear when the influence of unsteady trailing-edge separation on the wake structure diminishes. The increase of shear stress with downstream distance in Fig. 4d is also similar to the case of Fig. 4c.

The instantaneous angles of attack for the case of Figs. 1a and 1d are the same. The drastic differences between the flow patterns and the measurement data for these two cases are due to the flow history or hysteresis which is a most fundamental property of unsteady flows. Because of this hysteretic behavior, one should be cautious when comparison between the unsteady measurement data and the corresponding steady data are made.

The velocity profiles of the unsteady case and those of the steady case given in Fig. 2a are similar to one another. However, the unsteady and the steady profiles of Fig. 2d, where the instantaneous angle of attack is the same as that of Fig. 2a, are very much different from one another. The Reynolds shear stress profiles depicted in Figs. 4a and 4d compare similarly. A plausible explanation for this tendency can be given as follows. The instantaneous velocity and the shear stress profiles given in Figs. 2a and 4a, respectively, are the ones measured after the airfoil undergoes maximum instantaneous angle of attack (7.4 deg) in pitch-down stroke (see Fig. 1). Hence, the flow developed during this pitch-down motion would be detected by the measurement taken at the instant marked by (a) in Fig. 1. Since the time rate of change of angle of attack ($d\alpha/dt$) around the maximum incidence is smaller than at the other incidences, the flow at incidences around 7.4 deg is exposed for longer period at high angle of attack. Thus, the flow situation would be similar to the steady state as shown in Figs. 2a and 4a. On the contrary, the unsteady measurements taken at the instant marked by (d) in Fig. 1 reflect the flow conditions developed at an earlier time. Therefore, the unsteady and the steady data in Figs. 2d and 4d are very much different from one another.

Summary

Various components of the Reynolds stresses in the near wake behind a sinusoidally pitching airfoil in conjunction with the visualized wake flow at several phase angles of oscillation were reported. The present measurement data elucidate the link between the turbulent normal and shear stresses and the wake flow pattern represented by the streaklines. Velocity and the Reynolds stress data were presented for the following cases: the wake immediately after the unsteady separation, the fully turbulent wake, the relaminarizing wake, and the Karman vortex street-type wake.

Acknowledgments

Financial support for this research from the Korea Advanced Institute of Science and Technology via a fundamental research grant and from the Korea Science and Engineering Foundation through the Advanced Fluids Engineering Research Center at Pohang Institute of Science and Technology are deeply appreciated.

References

[1]Ho, C.-M., and Chen, S.-H., "Unsteady Wake of a Plunging Airfoil," *AIAA Journal*, Vol. 19, No. 11, 1981, pp. 1492–1494.

[2]De Ruyck, J., and Hirsch, C., "Instantaneous Turbulence Profiles in the Wake of an Oscillating Airfoil," *AIAA Journal*, Vol. 21, No. 5, 1983, pp. 641, 642.

[3]Kim, J. S., and Park, S. O., "Smoke Wire Visualizations of Unsteady Separation Over an Oscillating Airfoil," *AIAA Journal*, Vol. 26, No. 11, 1988, pp. 1408–1410.

[4]Park, S. O., Kim, J. S., and Lee, B. I., "Hot-Wire Measurements of Near Wakes Behind an Oscillating Airfoil," *AIAA Journal*, Vol. 28, No. 1, 1990, pp. 22–28.

[5]Kanevce, G., and Oka, S., "Correcting Hot-Wire Readings for Influence of Fluid Temperature Variations," *DISA Information*, No. 15, Oct. 1973, pp. 21–24.

[6]Champagne, F. H., and Sleicher, C. A., "Turbulence Measurements with Inclined Hot-Wires," *Journal of Fluid Mechanics*, Vol. 28, Pt. 2, 1967, pp. 177–182.